

# MIHash: Online Hashing with Mutual Information

Fatih Cakir\* Kun He\* Sarah Adel Bargal Stan Sclaroff

Department of Computer Science  
Boston University, Boston, MA

{fcakir, hekun, sbargal, sclaroff}@cs.bu.edu

## Abstract

Learning-based adaptive hashing methods are widely used for nearest neighbor retrieval. Recently, online hashing methods have demonstrated a good performance-complexity tradeoff by learning hash functions from streaming data. In this paper, we aim to advance the state-of-the-art for online hashing. We first address a key challenge that has often been ignored: the binary codes for indexed data must be recomputed to keep pace with updates to the hash functions. We propose an efficient quality measure for hash functions, based on an information-theoretic quantity, mutual information, and use it successfully as a criterion to eliminate unnecessary hash table updates. Next, we show that mutual information can also be used as an objective in learning hash functions, using gradient-based optimization. Experiments on image retrieval benchmarks (including a 2.5M image dataset) confirm the effectiveness of our formulation, both in reducing hash table recomputations and in learning high-quality hash functions.

## 1. Introduction

Hashing is a widely used approach for practical nearest neighbor search in many computer vision applications. It has been observed that adaptive hashing methods that learn to hash from data generally outperform data-independent hashing methods such as the classical Locality Sensitive Hashing [4]. In this paper, we focus on a relatively new family of adaptive hashing methods, namely *online* adaptive hashing methods [1, 2, 6, 11]. These techniques employ on-line learning in the presence of streaming data, and are appealing due to their low computational complexity and their ability to adapt to changes in the data distribution.

Despite recent progress, a key challenge has not been addressed in online hashing, which motivates this work: the binary representations, *i.e.* the hash table, may become outdated after a change in the hash mapping. To reflect the

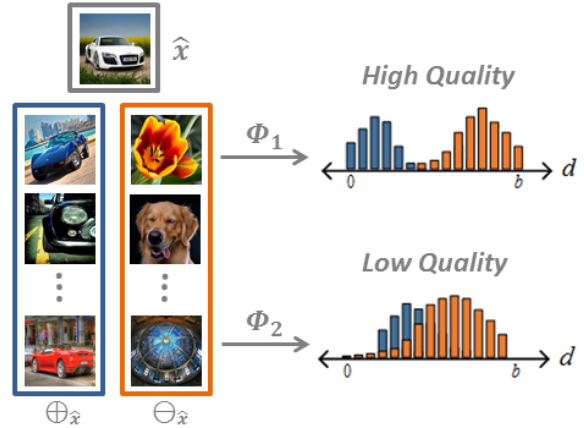


Figure 1: We study online hashing for efficient nearest neighbor retrieval. Given a hash mapping  $\Phi$ , an image  $\hat{x}$ , along with its neighbors in  $\oplus_{\hat{x}}$  and non-neighbors in  $\ominus_{\hat{x}}$ , are mapped to binary codes, yielding two distributions of Hamming distances. In this example,  $\Phi_1$  has higher quality than  $\Phi_2$  since it induces more separable distributions. The information-theoretic quantity Mutual Information can be used to capture the separability, which gives a good quality indicator and learning objective for online hashing.

updates in the hash mapping, the hash table may need to be recomputed frequently, causing inefficiencies in the system such as successive disk I/O, especially when dealing with large datasets. We thus identify an important question for online adaptive hashing systems: *when to update the hash table?* Previous online hashing solutions do not address this question, as they usually update both the hash mapping and hash table concurrently.

To answer the above question, we make the observation that achieving high quality nearest neighbor search is an ultimate goal in hashing systems, and therefore any effort to limit computational complexity should preserve, if not improve, that quality. Therefore, another important question is: *how to quantify quality?* Here, we briefly describe our answer to this question, but first introduce some necessary

\*First two authors contributed equally.

notation. We would like to learn a hash mapping  $\Phi$  from feature space  $\mathcal{X}$  to the  $b$ -dimensional Hamming space  $\mathcal{H}^b$ , whose outputs are  $b$ -bit binary codes. The goal of hashing is to preserve a neighborhood structure in  $\mathcal{X}$  after the mapping to  $\mathcal{H}^b$ . Given  $\hat{x} \in \mathcal{X}$ , the neighborhood structure is usually given in terms of a set of its neighbors  $\oplus_{\hat{x}}$ , and a set of non-neighbors  $\ominus_{\hat{x}}$ . We discuss how to derive the neighborhood structure in Sec. 3.

As shown in Fig. 1, the distributions of the Hamming distances from  $\hat{x}$  to its neighbors and non-neighbors are histograms over  $\{0, 1, \dots, b\}$ . Ideally, if there is no overlap between these two distributions, we can recover  $\oplus_{\hat{x}}$  and  $\ominus_{\hat{x}}$  by simply thresholding the Hamming distance. A nonzero overlap results in ambiguity, as observing the Hamming distance is no longer sufficient to determine neighbor relationships. Our discovery is that this overlap can be quantified using an information-theoretic quantity, *mutual information*, between two random variables induced by  $\Phi$ . We then use mutual information to define a novel measure to quantify quality for hash functions in general.

With a quality measure defined, we answer the motivating question of when to update the hash table. We propose a simple solution by restricting updates to times when there is an estimated improvement in hashing quality, based on an efficient estimation method in the presence of streaming data. Notably, since mutual information is a good general-purpose quality measure for hashing, this results in a general plug-in module for online hashing that does not require knowledge of the learning method.

Inspired by this strong result, a natural next question is, *can we optimize mutual information as an objective to learn hash functions?* We answer this by deriving gradient descent rules on the mutual information objective, which can then be used in online stochastic optimization. Mutual information is an appealing hash learning objective that is free of tuning parameters, unlike other formulations that may require thresholds, margins, *etc.*

We conduct experiments on three image retrieval benchmarks, including the Places205 dataset [32], which has 2.5M images. For four recent online hashing methods, our mutual information based update criterion consistently leads to over an order of magnitude reduction in hash table recomputations, while maintaining retrieval accuracy. Moreover, by optimizing the mutual information objective, our online hashing method achieves very competitive retrieval results compared to other online and batch hashing methods, including recent ones based on deep learning.

## 2. Related Work

In this section, we mainly review hashing methods that adaptively updates the hash mapping with incoming data, given that our focus is on online adaptive hashing. For a more general survey on hashing, please refer to [25].

Huang *et al.* [6] propose Online Kernel Hashing, where a stochastic environment is considered with pairs of points arriving sequentially in time. At each step, a number of hash functions are selected based on a Hamming loss measure and the parameters are updated via stochastic gradient descent (SGD).

Cakir and Sclaroff [1] argue that, in a stochastic setting, it is difficult to determine which hash functions to update as it is the collective effort of all the hash functions that yields a good hash mapping. Hamming loss is considered to infer the hash functions to be updated at each step and a squared error loss is minimized via SGD.

In [2], binary Error Correcting Output Codes (ECOCs) are employed in learning the hash functions. This work follows a more general two-step hashing framework [14], where the set of ECOCs are generated beforehand and are assigned to labeled data as they appear, allowing the label space to grow with incoming data. Then, hash functions are learned to fit the binary ECOCs using Online Boosting.

Inspired by the idea of “data sketching”, Leng *et al.* introduce Online Sketching Hashing [11] where a small fixed-size sketch of the incoming data is maintained in an online fashion. The sketch retains the Frobenius norm of the full data matrix, which offers space savings, and allows to apply certain batch-based hashing methods. A PCA-based batch learning method is applied on the sketch to obtain hash functions.

None of the above online hashing methods offer a solution to decide whether or not the hash table shall be updated given a new hash mapping. However, such a solution is crucial in practice, as limiting the frequency of updates will alleviate the computational burden of keeping the hash table up-to-date. Although [2] and [6] include strategies to select individual hash functions to recompute, they still require computing on all indexed data instances.

Recently, some methods employ deep neural networks to learn hash mappings, *e.g.* [12, 15, 27, 30] and others. These methods use minibatch-based stochastic optimization, however, they usually require multiple passes over a given dataset to learn the hash mapping, and the hash table is only computed when the hash mapping has been learned. Therefore, current deep learning based hashing methods are essentially batch learning methods, which differ from the online hashing methods that we consider, *i.e.* methods that process streaming data to learn and update the hash mappings on-the-fly while continuously updating the hash table. Nevertheless, when evaluating our mutual information based hashing objective, we compare against state-of-the-art batch hashing formulations as well, by contrasting different objective functions on the same model architecture.

Lastly, Ustinova *et al.* [23] recently proposed a method to derive differentiation rules for objective functions that require histogram binning, and apply it in learning deep em-

beddings. When optimizing our mutual information objective, we utilize their differentiable histogram binning technique for deriving gradient-based optimization rules. Note that both our problem setup and objective function are quite different from [23].

### 3. Online Hashing with Mutual Information

As mentioned in Sec. 1, the goal of hashing is to learn a hash mapping  $\Phi : \mathcal{X} \rightarrow \mathcal{H}^b$  such that a desired neighborhood structure is preserved. We consider an online learning setup where  $\Phi$  is continuously updated from input streaming data, and at time  $t$ , the current mapping  $\Phi_t$  is learned from  $\{\mathbf{x}_1, \dots, \mathbf{x}_t\}$ . We follow the standard setup of learning  $\Phi$  from pairs of instances with similar/dissimilar labels [9, 6, 1, 12]. These labels, along with the neighborhood structure, can be derived from a metric, *e.g.* two instances are labeled similar (*i.e.* neighbors of each other) if their Euclidean distance in  $\mathcal{X}$  is below a threshold. Such a setting is often called unsupervised hashing. On the other hand, in supervised hashing with labeled data, pair labels are derived from individual class labels: instances are similar if they are from the same class, and dissimilar otherwise.

Below, we first derive the mutual information quality measure and discuss its use in determining when to update the hash table in Sec. 3.1. We then describe a gradient-based approach for optimizing the same quality measure, as an objective for learning hash mappings, in Sec. 3.2. Finally, we discuss the benefits of using mutual information in Sec. 3.3.

#### 3.1. MI as Update Criterion

We revisit our motivating question: *When to update the hash table in online hashing?* During the online learning of  $\Phi_t$ , we assume a retrieval set  $\mathcal{S} \subseteq \mathcal{X}$ , which may include the streaming data after they are received. We define the hash table as the set of hashed binary codes:  $\mathcal{T}(\mathcal{S}, \Phi) = \{\Phi(\mathbf{x}) | \mathbf{x} \in \mathcal{S}\}$ . Given the adaptive nature of online hashing,  $\mathcal{T}$  may need to be recomputed often to keep pace with  $\Phi_t$ ; however, this is undesirable if  $\mathcal{S}$  is large or the change in  $\Phi_t$ 's quality does not justify the cost of an update.

We propose to view the learning of  $\Phi_t$  and computation of  $\mathcal{T}$  as separate events, which may happen at different rates. To this end, we introduce the notion of a *snapshot*, denoted  $\Phi^s$ , which is occasionally taken of  $\Phi_t$  and used to recompute  $\mathcal{T}$ . Importantly, this happens only when the nearest neighbor retrieval quality of  $\Phi_t$  has improved, and we now define the quality measure.

Given hash mapping  $\Phi : \mathcal{X} \rightarrow \{-1, +1\}^b$ ,  $\Phi$  induces Hamming distance  $d_\Phi : \mathcal{X} \times \mathcal{X} \rightarrow \{0, 1, \dots, b\}$  as

$$d_\Phi(\mathbf{x}, \hat{\mathbf{x}}) = \frac{1}{2} (b - \Phi(\mathbf{x})^\top \Phi(\hat{\mathbf{x}})). \quad (1)$$

Consider some instance  $\hat{\mathbf{x}} \in \mathcal{X}$ , and the sets containing neighbors and non-neighbors,  $\oplus_{\hat{\mathbf{x}}}$  and  $\ominus_{\hat{\mathbf{x}}}$ .  $\Phi$  induces

two conditional distributions,  $P(d_\Phi(\mathbf{x}, \hat{\mathbf{x}}) | \mathbf{x} \in \oplus_{\hat{\mathbf{x}}})$  and  $P(d_\Phi(\mathbf{x}, \hat{\mathbf{x}}) | \mathbf{x} \in \ominus_{\hat{\mathbf{x}}})$  as seen in Fig. 1, and it is desirable to have low overlap between them. To formulate the idea, for  $\Phi$  and  $\hat{\mathbf{x}}$ , define random variable  $\mathcal{D}_{\hat{\mathbf{x}}, \Phi} : \mathcal{X} \rightarrow \{0, 1, \dots, b\}$ ,  $\mathbf{x} \mapsto d_\Phi(\mathbf{x}, \hat{\mathbf{x}})$ , and let  $\mathcal{C}_{\hat{\mathbf{x}}} : \mathcal{X} \rightarrow \{0, 1\}$  be the membership indicator for  $\oplus_{\hat{\mathbf{x}}}$ . The two conditional distributions can now be expressed as  $P(\mathcal{D}_{\hat{\mathbf{x}}, \Phi} | \mathcal{C}_{\hat{\mathbf{x}}} = 1)$  and  $P(\mathcal{D}_{\hat{\mathbf{x}}, \Phi} | \mathcal{C}_{\hat{\mathbf{x}}} = 0)$ , and we can write the *mutual information* between  $\mathcal{D}_{\hat{\mathbf{x}}, \Phi}$  and  $\mathcal{C}_{\hat{\mathbf{x}}}$  as

$$\mathcal{I}(\mathcal{D}_{\hat{\mathbf{x}}, \Phi}; \mathcal{C}_{\hat{\mathbf{x}}}) = H(\mathcal{C}_{\hat{\mathbf{x}}}) - H(\mathcal{C}_{\hat{\mathbf{x}}} | \mathcal{D}_{\hat{\mathbf{x}}, \Phi}) \quad (2)$$

$$= H(\mathcal{D}_{\hat{\mathbf{x}}, \Phi}) - H(\mathcal{D}_{\hat{\mathbf{x}}, \Phi} | \mathcal{C}_{\hat{\mathbf{x}}}) \quad (3)$$

where  $H$  denotes (conditional) entropy. In the following, for brevity we will drop subscripts  $\Phi$  and  $\hat{\mathbf{x}}$ , and denote the two conditional distributions and the marginal  $P(\mathcal{D}_{\hat{\mathbf{x}}, \Phi})$  as  $p_{\mathcal{D}}^+$ ,  $p_{\mathcal{D}}^-$ , and  $p_{\mathcal{D}}$ , respectively.

By definition,  $\mathcal{I}(\mathcal{D}; \mathcal{C})$  measures the decrease in uncertainty in the neighborhood information  $\mathcal{C}$  when observing the Hamming distances  $\mathcal{D}$ . We claim that  $\mathcal{I}(\mathcal{D}; \mathcal{C})$  also captures how well  $\Phi$  preserves the neighborhood structure of  $\hat{\mathbf{x}}$ . If  $\mathcal{I}(\mathcal{D}; \mathcal{C})$  attains a high value, which means  $\mathcal{C}$  can be determined with low uncertainty by observing  $\mathcal{D}$ , then  $\Phi$  must have achieved good separation (*i.e.* low overlap) between  $p_{\mathcal{D}}^+$  and  $p_{\mathcal{D}}^-$ .  $\mathcal{I}$  is maximized when there is no overlap, and minimized when  $p_{\mathcal{D}}^+$  and  $p_{\mathcal{D}}^-$  are exactly identical. Recall, however, that  $\mathcal{I}$  is defined with respect to a single instance  $\hat{\mathbf{x}}$ ; therefore, for a general quality measure, we integrate  $\mathcal{I}$  over the feature space:

$$Q(\Phi) = \int_{\mathcal{X}} \mathcal{I}(\mathcal{D}_{\hat{\mathbf{x}}, \Phi}; \mathcal{C}_{\hat{\mathbf{x}}}) p(\hat{\mathbf{x}}) d\hat{\mathbf{x}}. \quad (4)$$

$Q(\Phi)$  captures the expected amount of separation between  $p_{\mathcal{D}}^+$  and  $p_{\mathcal{D}}^-$  achieved by  $\Phi$ , over all instances in  $\mathcal{X}$ .

In the online setting, given the current hash mapping  $\Phi_t$  and previous snapshot  $\Phi^s$ , it is then straightforward to pose the update criterion as

$$Q(\Phi_t) - Q(\Phi^s) > \theta, \quad (5)$$

where  $\theta$  is a threshold; a straightforward choice is  $\theta = 0$ . However, Eq. 4 is generally difficult to evaluate due to the intractable integral; in practice, we resort to Monte-Carlo approximations to this integral, as we describe next.

#### Monte-Carlo Approximation by Reservoir Sampling

We give a Monte-Carlo approximation of Eq. 4. Since we work with streaming data, we employ the Reservoir Sampling algorithm [24], which enables sampling from a stream or sets of large/unknown cardinality. With reservoir sampling, we obtain a *reservoir set*  $\mathcal{R} \triangleq \{\mathbf{x}_1^r, \dots, \mathbf{x}_K^r\}$  from the stream, which can be regarded as a finite sample from  $p(\mathbf{x})$ . We estimate the value of  $Q$  on  $\mathcal{R}$  as:

$$Q_{\mathcal{R}}(\Phi) = \frac{1}{|\mathcal{R}|} \sum_{\mathbf{x}^r \in \mathcal{R}} \mathcal{I}(\mathcal{D}_{\mathbf{x}^r, \Phi}; \mathcal{C}_{\mathbf{x}^r}). \quad (6)$$

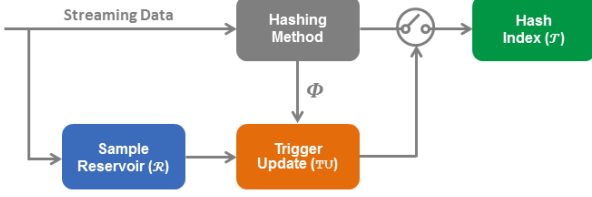


Figure 2: We present the general plug-in module for online hashing methods: Trigger Update (TU). We sample a reservoir  $\mathcal{R}$  from the input stream, and estimate the mutual information criterion  $Q_{\mathcal{R}}$ . Based on its value, TU decides whether a hash table update should be executed.

We use subscript  $\mathcal{R}$  to indicate that when computing the mutual information  $\mathcal{I}$ , the  $p_{\mathcal{D}}^+$  and  $p_{\mathcal{D}}^-$  for a reservoir instance  $\mathbf{x}^r$  are estimated from  $\mathcal{R}$ . This can be done in  $\mathcal{O}(|\mathcal{R}|)$  time for each  $\mathbf{x}^r$ , as the discrete distributions can be estimated via histogram binning.

Fig. 2 summarizes our approach. We use the reservoir set to estimate the quality  $Q_{\mathcal{R}}$ , and “trigger” an update to the hash table only when  $Q_{\mathcal{R}}$  improves over a threshold. Notably, our approach provides a general *plug-in module* for online hashing techniques, in that it only needs access to streaming data and the hash mapping itself, independent of the hashing method’s inner workings.

### 3.2. MI as Learning Objective

Having shown that mutual information is a suitable measure of neighborhood quality, we consider its use as a learning objective for hashing. Following the notation in Sec. 3.1, we define a loss  $\mathcal{L}$  with respect to  $\hat{\mathbf{x}} \in \mathcal{X}$  and  $\Phi$  as

$$\mathcal{L}(\hat{\mathbf{x}}, \Phi) = -\mathcal{I}(\mathcal{D}_{\hat{\mathbf{x}}, \Phi}; \mathcal{C}_{\hat{\mathbf{x}}}). \quad (7)$$

We model  $\Phi$  as a collection of parameterized hash functions, each responsible for generating a single bit:  $\Phi(\mathbf{x}) = [\phi_1(\mathbf{x}; W), \dots, \phi_b(\mathbf{x}; W)]$ , where  $\phi_i : \mathcal{X} \rightarrow \{-1, +1\}$ ,  $\forall i$ , and  $W$  represents the model parameters. For example, linear hash functions can be written as  $\phi_i(\mathbf{x}) = \text{sgn}(w_i^\top \mathbf{x})$ , and for deep neural networks the bits are generated by thresholding the activations of the output layer.

Inspired by the online nature of the problem and recent advances in stochastic optimization, we derive gradient descent rules for  $\mathcal{L}$ . The entropy-based mutual information is differentiable with respect to the entries of  $p_{\mathcal{D}}$ ,  $p_{\mathcal{D}}^+$  and  $p_{\mathcal{D}}^-$ , and, as mentioned before, these discrete distributions can be estimated via histogram binning. However, it is not clear how to differentiate histogram binning to generate gradients for model parameters. We describe a differentiable histogram binning technique next.

#### Differentiable Histogram Binning

We borrow ideas from [23] and estimate  $p_{\mathcal{D}}^+$ ,  $p_{\mathcal{D}}^-$  and  $p_{\mathcal{D}}$  using a differentiable histogram binning technique. For  $b$ -bit

Hamming distances, we use  $(K + 1)$ -bin normalized histograms with bin centers  $v_0 = 0, \dots, v_K = b$  and uniform bin width  $\Delta = b/K$ , where  $K = b$  by default. Consider, for example, the  $k$ -th entry in  $p_{\mathcal{D}}^+$ , denoted as  $p_{\mathcal{D},k}^+$ . It can be estimated as

$$p_{\mathcal{D},k}^+ = \frac{1}{|\oplus|} \sum_{\mathbf{x} \in \oplus} \delta_{\mathbf{x},k}, \quad (8)$$

where  $\delta_{\mathbf{x},k}$  records the contribution of  $\mathbf{x}$  to bin  $k$ . It is obtained by interpolating  $d_{\Phi}(\mathbf{x}, \hat{\mathbf{x}})$  using a triangular kernel:

$$\delta_{\mathbf{x},k} = \begin{cases} (d_{\Phi}(\mathbf{x}, \hat{\mathbf{x}}) - v_{k-1})/\Delta, & d_{\Phi}(\mathbf{x}, \hat{\mathbf{x}}) \in [v_{k-1}, v_k], \\ (v_{k+1} - d_{\Phi}(\mathbf{x}, \hat{\mathbf{x}}))/\Delta, & d_{\Phi}(\mathbf{x}, \hat{\mathbf{x}}) \in [v_k, v_{k+1}], \\ 0, & \text{otherwise.} \end{cases} \quad (9)$$

This binning process admits subgradients:

$$\frac{\partial \delta_{\mathbf{x},k}}{\partial d_{\Phi}(\mathbf{x}, \hat{\mathbf{x}})} = \begin{cases} 1/\Delta, & d_{\Phi}(\mathbf{x}, \hat{\mathbf{x}}) \in [v_{k-1}, v_k], \\ -1/\Delta, & d_{\Phi}(\mathbf{x}, \hat{\mathbf{x}}) \in [v_k, v_{k+1}], \\ 0, & \text{otherwise.} \end{cases} \quad (10)$$

#### Gradients of MI

We now derive the gradient of  $\mathcal{I}$  with respect to the output of the hash mapping,  $\Phi(\hat{\mathbf{x}})$ . Using standard chain rule, we can first write

$$\frac{\partial \mathcal{I}}{\partial \Phi(\hat{\mathbf{x}})} = \sum_{k=0}^K \left[ \frac{\partial \mathcal{I}}{\partial p_{\mathcal{D},k}^+} \frac{\partial p_{\mathcal{D},k}^+}{\partial \Phi(\hat{\mathbf{x}})} + \frac{\partial \mathcal{I}}{\partial p_{\mathcal{D},k}^-} \frac{\partial p_{\mathcal{D},k}^-}{\partial \Phi(\hat{\mathbf{x}})} \right]. \quad (11)$$

We focus on terms involving  $p_{\mathcal{D},k}^+$ , and omit derivations for  $p_{\mathcal{D},k}^-$  due to symmetry. For  $k = 0, \dots, K$ , we have

$$\frac{\partial \mathcal{I}}{\partial p_{\mathcal{D},k}^+} = -\frac{\partial H(\mathcal{D}|\mathcal{C})}{\partial p_{\mathcal{D},k}^+} + \frac{\partial H(\mathcal{D})}{\partial p_{\mathcal{D},k}^+} \quad (12)$$

$$= p^+(\log p_{\mathcal{D},k}^+ + 1) - (\log p_{\mathcal{D},k} + 1) \frac{\partial p_{\mathcal{D},k}}{\partial p_{\mathcal{D},k}^+} \quad (13)$$

$$= p^+(\log p_{\mathcal{D},k}^+ - \log p_{\mathcal{D},k}), \quad (14)$$

where we used the fact that  $p_{\mathcal{D},k} = p^+ p_{\mathcal{D},k}^+ + p^- p_{\mathcal{D},k}^-$ , with  $p^+$  and  $p^-$  being shorthands for the priors  $P(\mathcal{C} = 1)$  and  $P(\mathcal{C} = 0)$ . We next tackle the term  $\partial p_{\mathcal{D},k}^+ / \partial \Phi(\hat{\mathbf{x}})$  in Eq. 11.

From the definition of  $p_{\mathcal{D},k}^+$  in Eq.8, we have

$$\frac{\partial p_{\mathcal{D},k}^+}{\partial \Phi(\hat{\mathbf{x}})} = \frac{1}{|\oplus|} \sum_{\mathbf{x} \in \oplus} \frac{\partial \delta_{\mathbf{x},k}}{\partial \Phi(\hat{\mathbf{x}})} \quad (15)$$

$$= \frac{1}{|\oplus|} \sum_{\mathbf{x} \in \oplus} \frac{\partial \delta_{\mathbf{x},k}}{\partial d_{\Phi}(\mathbf{x}, \hat{\mathbf{x}})} \frac{\partial d_{\Phi}(\mathbf{x}, \hat{\mathbf{x}})}{\partial \Phi(\hat{\mathbf{x}})} \quad (16)$$

$$= \frac{1}{|\oplus|} \sum_{\mathbf{x} \in \oplus} \frac{\partial \delta_{\mathbf{x},k}}{\partial d_{\Phi}(\mathbf{x}, \hat{\mathbf{x}})} \frac{-\Phi(\mathbf{x})}{2}. \quad (17)$$

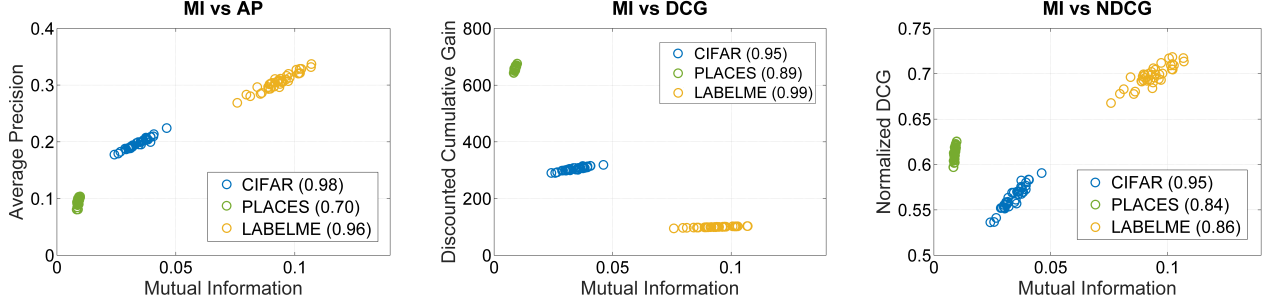


Figure 3: We show Pearson correlation coefficients between mutual information and AP, DCG, and NDCG, evaluated on the CIFAR-10, LabelMe, and Places205 datasets. The hash mapping parameters are sampled from a Gaussian, similar to LSH [4]. We sample 100 instances to form the query set, and use the rest to populate the hash table. Each experiment is conducted 50 times. MI corresponds to the mean mutual information over the query set.

Note that  $\partial \delta_{\mathbf{x},k} / \partial d_{\Phi}(\mathbf{x}, \hat{\mathbf{x}})$  is already given in Eq. 10. For the last step, we used the definition of  $d_{\Phi}$  in Eq. 1.

Lastly, to back-propagate gradients to  $\Phi$ 's inputs and ultimately model parameters, we approximate the discontinuous sign function with sigmoid, which is a standard technique in hashing, *e.g.* [1, 12, 16].

### 3.3. Benefits of MI

Hashing algorithms are often evaluated with standard ranking metrics, such as Average Precision (AP), Discounted Cumulative Gain (DCG), and Normalized DCG (NDCG) [17]. It is reasonable to question the use of mutual information, when the performance of a hashing system can be monitored directly by such metrics, as they too can be estimated on a reservoir set. We respond to this question by discussing the benefits of using mutual information.

First, we point out the lower computational complexity of mutual information. Let  $n$  be the reservoir set size. Computing Eq. 6 involves estimating discrete distributions via histogram binning, and takes  $\mathcal{O}(n)$  time for each reservoir item, since  $\mathcal{D}$  only takes discrete values from  $\{0, 1, \dots, b\}$ . In contrast, ranking measures such as AP and NDCG have  $\mathcal{O}(n \log n)$  complexity due to sorting, which render them disadvantageous for large  $n$ , for example when a large reservoir set is required for better approximation.

We also empirically show that there are strong correlations between mutual information and standard ranking metrics. Fig. 3 demonstrates the Pearson correlation coefficients between MI and AP, DCG, and NDCG, for random hash mappings on three benchmark datasets. Although a theoretical analysis is beyond the scope of this work, in practice we find that MI serves as an efficient and general-purpose ranking surrogate.

Finally, Sec. 3.2 showed that the mutual information objective is suitable for direct, gradient-based optimization. In contrast, optimizing metrics like AP and NDCG is more challenging as they are often non-differentiable or discon-

tinuous. Existing works resort to optimizing surrogates [13, 26, 29], as it is unclear how to directly apply gradient-based optimization. Furthermore, mutual information itself is essentially parameter-free, whereas many other hashing formulations require and could be sensitive to tuning parameters, such as thresholds or margins [18, 27], quantization strength [12, 15, 20], *etc.*

## 4. Experiments

We evaluate our approach on three widely used image benchmarks. We first describe the datasets and experimental setup in Sec. 4.1. We evaluate the mutual information update criterion in Sec. 4.2 and the mutual information based objective function for learning hash mappings in Sec. 4.3. Our implementations will be publicly available.

### 4.1. Datasets and Experimental Setup

**CIFAR-10** is a widely-used dataset for image classification and retrieval, containing 60K images from 10 different categories [7]. For feature representation, we use CNN features extracted from the *fc7* layer of a VGG-16 network [21] pre-trained on ImageNet [3].

**Places205** is a subset of the large-scale Places dataset [32] for scene recognition. Places205 contains 2.5M images from 205 scene categories. This is a very challenging dataset due to its large size and number of categories, and it has not been studied in the hashing literature to our knowledge. We extract CNN features from the *fc7* layer of an AlexNet [8] pre-trained on ImageNet, and reduce the dimensionality to 128 using PCA.

**LabelMe.** The 22K LabelMe dataset [19, 22] has 22,019 images represented as 512-dimensional GIST descriptors. This is an unsupervised dataset without labels, and standard practice uses the Euclidean distance to determine neighbor relationships. Specifically,  $\mathbf{x}_i$  and  $\mathbf{x}_j$  are considered neighbor pairs if their Euclidean distance is within the smallest

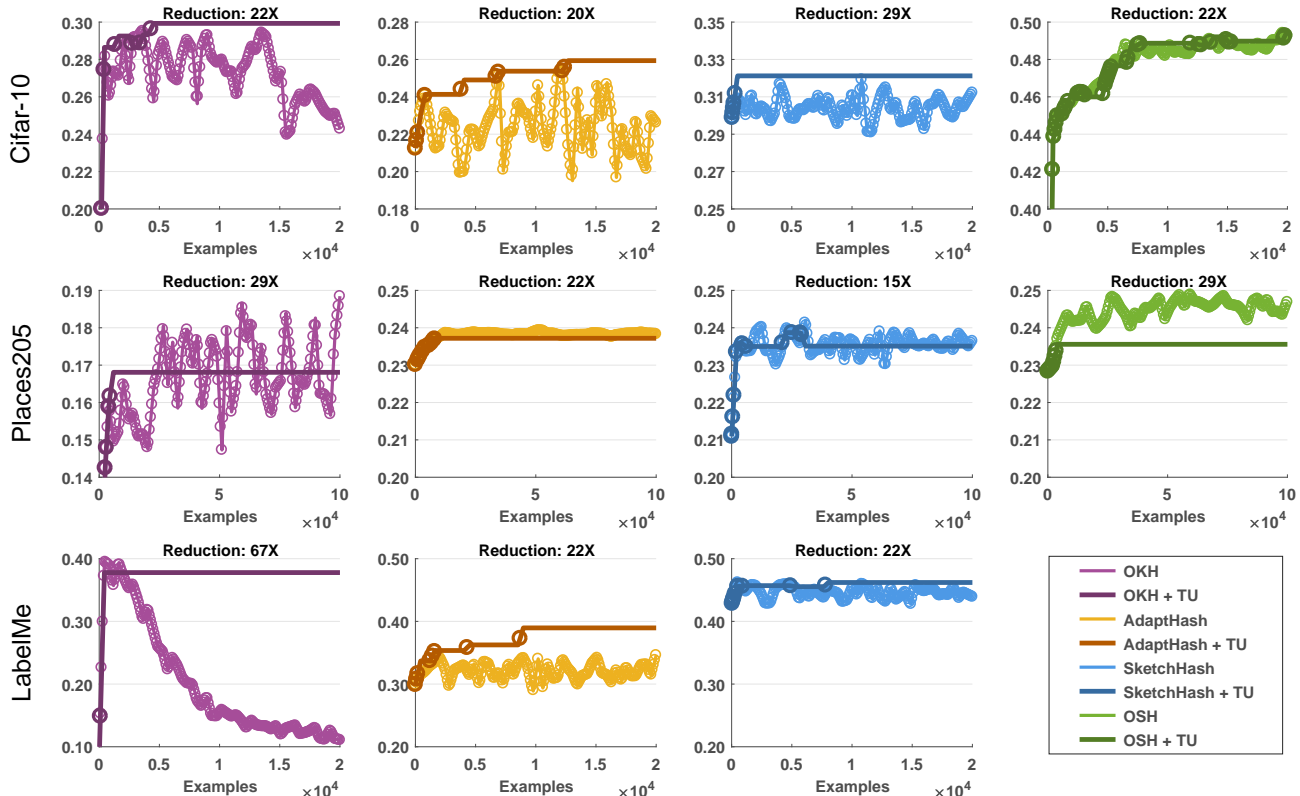


Figure 4: Retrieval mAP vs. number of training examples over time (as the method processes the streaming training data) for four hashing methods on the three datasets, with and without Trigger Update (TU). We use default threshold  $\theta = 0$  for TU. Circles indicate hash table updates, and the ratio of reduction in the number of updates is marked for each graph. TU substantially reduces the number of updates while having a stabilizing effect on the retrieval performance. Note: since the OSH method [2] assumes supervision in terms of class labels, it is not applicable to the unsupervised LabelMe dataset.

5% in the training set. For a query, the closest 5% examples are considered true neighbors.

All datasets are randomly split into a retrieval set and a test set, and a subset from the retrieval set is used for learning hash functions. Specifically, for **CIFAR-10**, the test set has 1K images and the retrieval set has 59K. A random subset of 20K images from the retrieval set is used for learning, and the size of the reservoir is set to 1K. For **Places205**, we sample 20 images from each class to construct a test set of 4.1K images, and use the rest as the retrieval set. A random subset of 100K images is used for learning, and the reservoir size is 5K. For **LabelMe**, the dataset is split into retrieval and test sets with 20K and 2K samples, respectively. Similar to CIFAR-10, we use a reservoir of size 1K.

To evaluate the retrieval performance we use mean Average Precision (mAP), which has been widely employed in evaluating hashing algorithms. For Places205, mAP is very time-consuming to compute due to its large size. We compute mAP only on the top 1000 retrieved examples (mAP@1000), as also done in [15] for other datasets.

For online hashing experiments, we run three randomized trials for each experiment and average the results, where the random splits and ordering of the training sequence are all different in each trial.

## 4.2. Evaluation: Update Criterion

We evaluate our mutual information based update criterion, the Trigger Update module (TU). We apply TU to all existing online hashing methods known to us: Online Kernel Hashing (OKH) [6], Online Supervised Hashing (OSH) [2], Adaptive Hashing (AdaptHash) [1] and Online Sketching Hashing (SketchHash) [11]. We use publicly available implementations of all methods.

For these experiments, we fix the code length to 32 bits. For each method, we create a corresponding data-agnostic baseline that updates the hash table at a fixed rate, controlled by parameter  $U$ . After processing every  $U$  examples, the baseline triggers an update, while TU makes a decision using the mutual information criterion. For each dataset,  $U$  is set such that the baseline updates 201 times in total.



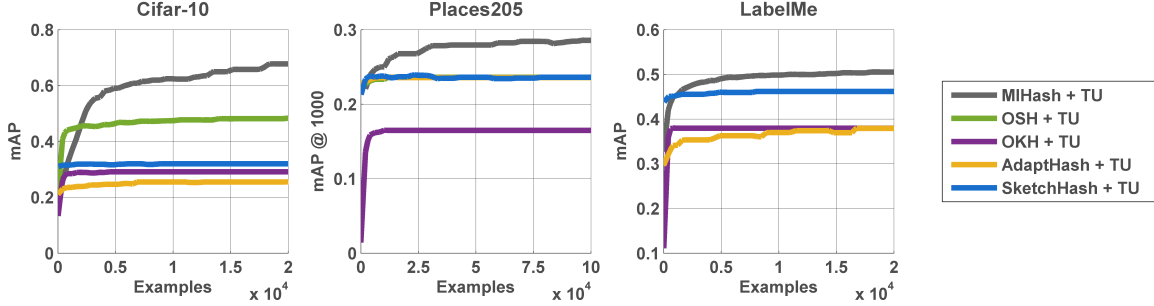


Figure 5: Online hashing performance (mAP) comparison on three datasets, where all methods use the Trigger Update module (TU) with  $\theta = 0$ . Using the mutual information objective, MIHash clearly outperforms other competing methods. OSH, AdaptHash, and SketchHash perform very similarly on Places205, thus their curves overlap.

**Results for the Trigger Update module.** Fig. 4 depicts the retrieval mAP over time for all four online hashing methods considered, on three datasets, with and without incorporating TU. We can clearly observe a significant reduction in the number of hash table updates, between one and two orders of magnitude in all cases. For example, the number of hash table updates is reduced by a factor of 67 for the OKH method on LabelMe, and the smallest reduction factor is 15, for SketchHash on the Places205 dataset.

The quality-based update criterion is particularly important for hashing methods that may yield inferior hash mappings due to noisy data and/or imperfect learning techniques. In other words, TU can be used to *filter* updates to the hash mapping with negative or small improvement. This has a stabilizing effect on the mAP curve, notably for OKH and AdaptHash. For OSH, which appears to stably improve over time, TU nevertheless significantly reduces revisits to the hash table while maintaining its performance.

All results in Fig. 4 are obtained using the default threshold parameter  $\theta = 0$ , defined in Eq. 5. We do not tune  $\theta$  in order to show general applicability. We also discuss the impact of the reservoir set  $\mathcal{R}$ . There is a trade-off regarding the size of  $\mathcal{R}$ ; a larger  $\mathcal{R}$  leads to better approximation but increases computation. Nevertheless, we observed robust and consistent results with  $|\mathcal{R}|$  not exceeding 5% of the size of the training stream.

### 4.3. Evaluation: Learning Objective

We evaluate the mutual information based hashing objective. We name our model using the mutual information objective MIHash, and train it using stochastic gradient descent (SGD). This allows it to be applied to both the online setting and batch setting in learning hash functions.

During minibatch-based SGD, to compute the mutual information objective in Eq. 7 and its gradients, we need access to the sets  $\oplus_{\hat{x}}$ ,  $\ominus_{\hat{x}}$  for each considered  $\hat{x}$ , in order to estimate  $p_{\mathcal{D}}^+$  and  $p_{\mathcal{D}}^-$ . For the online setting in Sec. 4.3.1, a standalone reservoir set  $\mathcal{R}$  is assumed as in the previous experiment, and we partition  $\mathcal{R}$  into  $\{\oplus_{\hat{x}}, \ominus_{\hat{x}}\}$  with respect to

each incoming  $\hat{x}$ . In this case a batch size of 1 can be used. For the batch setting in Sec. 4.3.2, for each  $\hat{x}$  in a minibatch,  $\{\oplus_{\hat{x}}, \ominus_{\hat{x}}\}$  are defined within the same minibatch.

#### 4.3.1 Online Setting

We first consider an online setting that is the same as in Sec. 4.2. We compare against other online hashing methods: OKH, OSH, AdaptHash and SketchHash. All methods are equipped with the TU module with  $\theta = 0$ , which has been demonstrated to work well.

**Results for Online Setting.** We first show the mAP curve comparisons in Fig. 5. For competing online hashing methods, the curves are the same as the ones with TU in Fig. 4, and we remove markers to avoid clutter. MIHash clearly outperforms other online hashing methods on all three datasets, and shows potential for further improvement with more data, as the mAP curves are not saturated. The combination of TU and MIHash gives a complete online hashing system that enjoys a superior learning objective with a plug-in update criterion that improves efficiency.

We next give insights into the distribution-separating effect from optimizing mutual information. In Fig. 6, we plot the conditional distributions  $p_{\mathcal{D}}^+$  and  $p_{\mathcal{D}}^-$  averaged on the CIFAR-10 test set, before and after learning MIHash with the 20K training examples. Before learning, with a randomly initialized hash mapping,  $p_{\mathcal{D}}^+$  and  $p_{\mathcal{D}}^-$  exhibit high overlap. After learning, MIHash achieves good separation between  $p_{\mathcal{D}}^+$  and  $p_{\mathcal{D}}^-$ : the overlap reduces significantly, and  $p_{\mathcal{D}}^+$ 's mass is pushed towards 0. The separation is reflected in the large improvement in mAP.

In contrast with the other methods, our mutual information formulation is parameter-free. For instance, there is no threshold parameter that requires separating  $p_{\mathcal{D}}^+$  and  $p_{\mathcal{D}}^-$  at a certain distance value. Likewise, there is no margin parameter that dictates the amount of separation in absolute terms. Parameters as such usually need to be tuned to fit to data, whereas the optimization of mutual information is automatically guided by the data itself.

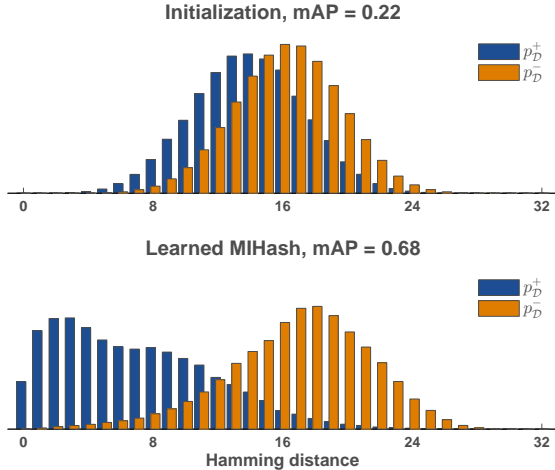


Figure 6: The distribution separating effect of mutual information. We estimate and average the distributions  $p_D^+$  and  $p_D^-$ , on the CIFAR-10 test set, before and after learning MIHash with the 20K training examples. Optimizing the mutual information objective successfully reduces the overlap, and achieves state-of-the-art mAP for the online setting, as shown in Fig. 5.

#### 4.3.2 Batch Setting

To further demonstrate the potential of MIHash, we consider the batch learning setting, and compare against state-of-the-art batch formulations. The methods include: Supervised Hashing with Kernels (SHK) [16], Fast Supervised Hashing with Decision Trees (FastHash) [14], Supervised Discrete Hashing (SDH) [20], Efficient Training of Very Deep Neural Networks (VDSH) [30], Deep Supervised Hashing with Pairwise Labels (DPSH) [12] and Deep Supervised Hashing with Triplet Labels (DTSH) [27]. We focus on comparisons on the CIFAR-10 dataset, which is the canonical benchmark for supervised hashing. These competing methods have shown to outperform earlier and other work such as [5, 9, 18, 28, 10, 31].

Our goal is to contrast different learning objectives, and for fair and efficient comparisons, we restrict all models to use the same underlying network, VGG-16 [21], pretrained on ImageNet. For MIHash and two deep hashing methods (DPSH, DTSH), the last fully connected layer is finetuned to produce hash codes according to each method’s objective. Although performance can be improved by finetuning the entire network, that is not our focus when comparing learning objectives. For VDSH, we use the full model with 16 layers and 1024 nodes per layer. In SHK, FastHash, and SDH, this setup corresponds to using VGG-16 features in their respective formulations.

We follow the experimental setup in [10, 12, 27], which uses 5K training examples to learn hash mappings. As standard practice, we report mAP values for hash code lengths

Method	Code Length			
	12 Bits	24 Bits	32 Bits	48 Bits
SHK [16]	0.497	0.615	0.645	0.682
SDH [20]	0.521	0.576	0.589	0.592
FastHash [14]	<u>0.632</u>	<u>0.70</u>	<u>0.724</u>	<u>0.738</u>
VDSH* [30]	0.523	0.546	0.537	0.554
DPSH [12]	0.42	0.518	0.538	0.553
DTSH [27]	0.617	0.659	0.689	0.702
MIHash, 1ep	0.524	0.563	0.597	0.609
MIHash	<b>0.683</b>	<b>0.720</b>	<b>0.727</b>	<b>0.746</b>

Table 1: Retrieval mAP for batch hashing methods on the CIFAR-10 dataset using VGG-16. Models with an asterisk (\*) are trained with the full model. 1ep stands for training for one epoch only. **Bold** and underlined results are the best and second best for each column, respectively.

12, 24, 32 and 48 on CIFAR-10. We use the publicly available code for the comparisons and exhaustively search parameter settings including the default parameters as provided by the authors. We give details for compared methods in the supplementary material.

All methods are trained to convergence with multiple epochs over the 5K training set. For MIHash, the batch size is set to 100. We also report results after training MIHash for a single epoch.

**Results for Batch Setting.** In Table 1, we list results for all methods. We first note that MIHash outperforms competing deep hashing methods (VDSH, DPSH, DTSH) significantly, in some cases only using a single training epoch. This suggests that the mutual information objective is a more effective learning objective for learning hash functions. Such a comparison is fair, since by finetuning the final layer of VGG-16, all these methods essentially learn linear hash functions using the same input features.

Next we discuss the other methods in Table 1: SHK, SDH, and FastHash. These methods learn non-linear hash functions on the input VGG-16 features, which allows them to generally outperform MIHash trained for a single epoch. But given sufficient training, MIHash achieves better results at convergence. Note that the closest competitor, FastHash, is a two-step hashing method based on sophisticated binary code inference and boosted trees, while MIHash directly learns linear hash functions.

## 5. Conclusion

We advance the state-of-the-art for online hashing in this paper. Motivated by the issue of hash table updates in online hashing, we propose to explore quality-based update criteria, and define a quality measure using the mutual information between variables induced by the hash mapping. This quality measure is efficiently computable and highly correlates with standard ranking metrics, and leads to consistent reduction in hash table updates for four online hashing



methods on three benchmark datasets, while maintaining retrieval accuracy. Inspired by these strong results, we further propose a hashing method MIHash, by optimizing mutual information as an objective with gradient descent. In both online and batch settings, MIHash achieves superior performance compared to state-of-the-art hashing techniques.

## References

- [1] F. Cakir and S. Sclaroff. Adaptive hashing for fast similarity search. In *Proc. IEEE International Conf. on Computer Vision (ICCV)*, 2015.
- [2] F. Cakir and S. Sclaroff. Online supervised hashing. In *Proc. IEEE International Conf. on Image Processing (ICIP)*, 2015.
- [3] J. Deng, W. Dong, R. Socher, L.-J. Li, K. Li, and L. Fei-Fei. Imagenet: A large-scale hierarchical image database. In *CVPR*, 2009.
- [4] A. Gionis, P. Indyk, and R. Motwani. Similarity search in high dimensions via hashing. In *Proc. International Conf. on Very Large Data Bases (VLDB)*, 1999.
- [5] Y. Gong and S. Lazebnik. Iterative quantization: A procrustean approach to learning binary codes. In *Proc. IEEE Conf. on Computer Vision and Pattern Recognition (CVPR)*, 2011.
- [6] L.-K. Huang, Q. Y. Yang, and W.-S. Zheng. Online hashing. In *Proc. International Joint Conf. on Artificial Intelligence (IJCAI)*, 2013.
- [7] A. Krizhevsky and G. Hinton. Learning multiple layers of features from tiny images, 2009.
- [8] A. Krizhevsky, I. Sutskever, and G. E. Hinton. Imagenet classification with deep convolutional neural networks. In *Proc. Advances in Neural Information Processing Systems (NIPS)*, 2012.
- [9] B. Kulis and T. Darrell. Learning to hash with binary reconstructive embeddings. In *Proc. Advances in Neural Information Processing Systems (NIPS)*, 2009.
- [10] H. Lai, Y. Pan, Y. Liu, and S. Yan. Simultaneous feature learning and hash coding with deep neural networks. In *Proc. IEEE Conf. on Computer Vision and Pattern Recognition (CVPR)*, 2015.
- [11] C. Leng, J. Wu, J. Cheng, X. Bai, and H. Lu. Online sketching hashing. In *Proc. IEEE Conf. on Computer Vision and Pattern Recognition (CVPR)*, 2015.
- [12] W.-J. Li, S. Wang, and W.-C. Kang. Feature learning based deep supervised hashing with pairwise labels. In *Proc. International Joint Conf. on Artificial Intelligence (IJCAI)*, 2016.
- [13] G. Lin, F. Liu, C. Shen, J. Wu, and H. T. Shen. Structured learning of binary codes with column generation for optimizing ranking measures. *International Journal of Computer Vision (IJCV)*, pages 1–22, 2016.
- [14] G. Lin, C. Shen, Q. Shi, A. van den Hengel, and D. Suter. Fast supervised hashing with decision trees for high-dimensional data. In *Proc. IEEE Conf. on Computer Vision and Pattern Recognition (CVPR)*, 2014.
- [15] K. Lin, J. Lu, C.-S. Chen, and J. Zhou. Learning compact binary descriptors with unsupervised deep neural networks. In *Proc. IEEE Conf. on Computer Vision and Pattern Recognition (CVPR)*, 2016.
- [16] J. W. Liu, Wei and, R. Ji, Y.-G. Jiang, and S.-F. Chang. Supervised hashing with kernels. In *Proc. IEEE Conf. on Computer Vision and Pattern Recognition (CVPR)*, 2012.
- [17] C. D. Manning, P. Raghavan, and H. Schütze. Introduction to information retrieval. 2008.
- [18] M. Norouzi and D. J. Fleet. Minimal loss hashing for compact binary codes. In *Proc. International Conf. on Machine Learning (ICML)*, 2011.
- [19] B. C. Russell, A. Torralba, K. P. Murphy, and W. T. Freeman. Labelme: a database and web-based tool for image annotation. *International journal of computer vision*, 2008.
- [20] F. Shen, C. S. Wei, L. Heng, and T. Shen. Supervised discrete hashing. In *Proc. IEEE Conf. on Computer Vision and Pattern Recognition (CVPR)*, 2015.
- [21] K. Simonyan and A. Zisserman. Very deep convolutional networks for large-scale image recognition. *ICLR*, 2015.
- [22] A. Torralba, R. Fergus, and Y. Weiss. Small codes and large image databases for recognition. In *Proc. IEEE Conf. on Computer Vision and Pattern Recognition (CVPR)*. IEEE, 2008.
- [23] E. Ustinova and V. Lempitsky. Learning deep embeddings with histogram loss. In *Proc. Advances in Neural Information Processing Systems (NIPS)*, pages 4170–4178, 2016.
- [24] J. S. Vitter. Random sampling with a reservoir. *ACM Transactions on Mathematical Software (TOMS)*, 11(1):37–57, 1985.
- [25] J. Wang, H. T. Shen, J. Song, and J. Ji. Hashing for similarity search: A survey. *CoRR*.
- [26] Q. Wang, Z. Zhang, and L. Si. Ranking preserving hashing for fast similarity search. In *Proc. International Joint Conf. on Artificial Intelligence (IJCAI)*, 2015.
- [27] Y. Wang, Xiaofang Shi and K. M. Kitani. Deep supervised hashing with triplet labels. In *Proc. Asian Conf. on Computer Vision (ACCV)*, 2016.
- [28] R. Xia, Y. Pan, H. Lai, C. Liu, and S. Yan. Supervised hashing for image retrieval via image representation learning. In *Proc. AAAI Conf. on Artificial Intelligence (AAAI)*, volume 1, page 2, 2014.
- [29] Y. Yue, T. Finley, F. Radlinski, and T. Joachims. A support vector method for optimizing average precision. In *Proc. ACM Conf. on Research & Development in Information Retrieval (SIGIR)*, pages 271–278. ACM, 2007.
- [30] Z. Zhang, Y. Chen, and V. Saligrama. Efficient training of very deep neural networks for supervised hashing. In *Proc. IEEE Conf. on Computer Vision and Pattern Recognition (CVPR)*, 2016.
- [31] F. Zhao, Y. Huang, L. Wang, and T. Tan. Deep semantic ranking based hashing for multi-label image retrieval. In *Proc. IEEE Conf. on Computer Vision and Pattern Recognition (CVPR)*, 2015.
- [32] B. Zhou, A. Lapedriza, J. Xiao, A. Torralba, and A. Oliva. Learning deep features for scene recognition using places database. In *Proc. Advances in Neural Information Processing Systems (NIPS)*, 2014.

## Appendix

### A. Implementation Details of MIHash

We discuss the implementation details of MIHash. In the online hashing experiments, for simplicity we model MIHash using linear hash functions, in the form of  $\phi_i(\mathbf{x}) = \text{sgn}(w_i^\top \mathbf{x}) \in \{-1, +1\}$ ,  $i = 1, \dots, b$ . The learning capacity of such a model is lower than the kernel-based OKH, and is the same as OSH, AdaptHash, and SketchHash, which use linear hash functions as well.

For the batch hashing experiments, as mentioned in Sec. 4.3.2, for MIHash as well as other competing deep hashing methods, we take a VGG-16 network pretrained on ImageNet, replace the original output layer with a fully connected layer that has the same number of outputs as the hash bits, and learn this layer. This also amounts to learning linear hash functions using *fc7* features from VGG-16.

We train MIHash using stochastic gradient descent. In Eq. 11, we gave the gradients of the mutual information objective  $\mathcal{I}$  with respect to the *outputs* of the hash mapping,  $\Phi(\mathbf{x})$ . Both  $\mathcal{I}$  and  $\partial\mathcal{I}/\partial\Phi(\mathbf{x})$  are parameter-free. In order to further back-propagate gradients to the *inputs* of  $\Phi(\mathbf{x})$  and model parameters  $\{w_i\}$ , we approximate the  $\text{sgn}$  function using the sigmoid function  $\sigma$ :

$$\phi_i(\mathbf{x}) \approx 2\sigma(Aw_i^\top \mathbf{x}) - 1, \quad (18)$$

where  $A > 1$  is a scaling parameter, used to increase the “sharpness” of the approximation. We find  $A$  from the set  $\{5, 10, 20, 50\}$  in our experiments.

We note that  $A$  is not a tuning parameter of the mutual information objective, but rather a parameter of the underlying hash functions. The design of the hash functions is independent of the mutual information objective and can be separated. It will be an interesting topic to explore other methods of constructing hash functions, potentially in ways that are free of tuning parameters.

### B. Experimental Details

#### B.1. The streaming scenario

We set up a streaming scenario in our online hashing experiments. We run three randomized trials for each experiment. In each trial, we first randomly split the dataset into a retrieval set and a test set as described in Sec. 4.1, and randomly sample the training subset from the retrieval set. The ordering of the training set is also randomly permuted. The random seeds are fixed, so the baselines and methods with the Trigger Update module observe the same training sequences.

In a streaming setting, we also measure the *cumulative* retrieval performance during online hashing, as opposed to only the final results. To mimic real retrieval systems where

queries arrive randomly, we set 50 randomized checkpoints during the online process. We first place the checkpoints with equal spacing, then add small random perturbations to their locations. We measure the instantaneous retrieval mAP at these checkpoints to get mAP vs. time curves (*e.g.* curves shown in Fig. 5), and compute the area under curve (AUC). AUC gives a summary of the entire online learning process, which cannot be reflected by the final performance at the end.

#### B.2. Parameters for online hashing methods

We describe parameters used for online hashing methods in the online experiments. Some of the competing methods require parameter tuning, therefore we sample a validation set from the training data and find the best performing parameters for each method. The size of the validation sets are 2K, 2K and 10K for CIFAR-10, LabelMe and Places205, respectively. Please refer to the respective papers for the descriptions of the parameters.

- **OKH** [6]: the tuple  $(C, \alpha)$  is set to  $(0.001, 0.3)$ ,  $(0.001, 0.3)$  and  $(0.0001, 0.7)$  for CIFAR-10, LabelMe and Places205, respectively.
- **OSH** [2]:  $\eta$  is set to 0.1 for all datasets. The ECOC codebook  $C$  is populated the same way as in OSH.
- **AdaptHash** [1]: the tuple  $(\alpha, \lambda, \eta)$  is set to  $(0.9, 0.01, 0.1)$ ,  $(0.1, 0.01, 0.001)$  and  $(0.9, 0.01, 0.1)$  for CIFAR-10, LabelMe and Places205, respectively.
- **SketchHash** [11]: the pair (sketch size, batch size) is set to  $(200, 50)$ ,  $(100, 50)$  and  $(100, 50)$  for CIFAR-10, LabelMe and Places205, respectively.

#### B.3. Parameters for batch hashing methods

We use the publicly available implementations for the compared methods, and exhaustively search parameter settings including the default parameters as provided by the authors. For DPSH [12] and DTSH [27], we found a setting that worked well for all evaluated hash code lengths: the mini-batch size is set to the default value of 128, and the learning rate is initialized to 1 and decayed by a factor of 0.9 after every 20 epochs. Additionally, for DTSH, the margin parameter is set to  $b/4$  where  $b$  is the hash code length. VDSH [30] uses a heavily customized architecture with only fully-connected layers, and it is unclear how to adapt it to work with standard CNN architectures. In this sense, VDSH is more akin to nonlinear hashing methods such as FastHash [14] and SHK [16]. We used the full VDSH model with 16 layers and 1024 nodes per layer, and found the default parameters to perform the best, except that we increased the number of training iterations by an order of magnitude during finetuning.

Method	Training Time (s)
OKH [6]	10.8
OKH + TU	23.6
OSH [2]	97.6
OSH + TU	175.8
AdaptHash [1]	47.8
AdaptHash + TU	94.8
SketchHash [11]	68.8
SketchHash + TU	80.0

Table 2: Online hashing: running times on the CIFAR-10 20k training set, with 32-bit hash codes. For methods with the TU plugin, the added time is due to maintaining the reservoir set and computing the mutual information update criterion, and is dominated by the maintaining of the reservoir set.

As stated before, all methods are trained to convergence with multiple epochs over the 5K training set. For MIHash, we use a batch size of 100, and run SGD with initial learning rate of 0.1 and a decay factor of 0.5 every 10 epochs, for 100 epochs.

## C. Running Time

### C.1. Online Setting: Trigger Update Module

In Table 2 we report running time for all methods on the CIFAR-10 dataset with 20k training examples, including time spent in learning hash functions and the added processing time for maintaining the reservoir set and computing TU. Numbers are recorded on a 2.3GHz Intel Xeon E5-2650 CPU workstation with 128GB of DDR3 RAM. Most of the added time is due to maintaining the reservoir set, which is invoked in each training iteration; the mutual information update criterion is only checked after processing every  $U = 100$  examples. Methods with small batch sizes (*e.g.* OSH, batch size 1) therefore incur more overhead than methods with larger batches (*e.g.* SketchHash, batch size 50). Results for other datasets are similar.

We note that in a real retrieval system with large-scale data, the bottleneck likely lies in recomputing the hash tables for indexed data, due to various factors such as scheduling and disk I/O. We reduce this bottleneck significantly by using TU. Compared to this bottleneck, the increased training time is likely not significant.

### C.2. Batch Setting

Table 3 reports CPU times for learning 48-bit hash mappings for all batch hashing methods, on the CIFAR-10 5k training set. The retrieval mAP numbers are replicated from Table 1. Our current Matlab implementation of MIHash achieves 1.9 seconds per epoch on CPU. MIHash achieves competitive performance with a single

Method	mAP	Training Time (s)
SHK [16]	0.682	180
SDH [20]	0.592	4.8
FastHash [14]	0.738	140
VDSH* [30]	0.554	206
DPSH [12]	0.553	450
DTSH [27]	0.702	1728
MIHash, 1ep	0.609	1.9
MIHash	0.746	190

Table 3: Batch hashing: test performance and training time for 48-bit codes on the CIFAR-10, using the 5k training set. \*VDSH is trained with the full model as detailed in B.3. 1ep stands for training for one epoch only.

epoch, and has a total training time on par with FastHash, while yielding superior performance.

## D. Additional Experimental Results

### D.1. Online Hashing: Other Code Lengths

In Sec. 4, we reported online hashing experiments where all methods are compared in the same setup with 32-bit hash codes. Additionally, we present results using 64-bit hash codes on all three datasets. The parameters for all methods are found through validation as described in B.2.

Similar to Sec 4.2 and 4.3.1, we show the comparisons with and without TU for existing online hashing methods in Fig. 7, and plot the mAP curves for all methods, including MIHash, in Fig. 8. The 64-bit results are uniformly better than 32-bit results for all methods in terms of mAP, but still follow the same patterns. Again, we can see that MIHash clearly outperforms all competing online hashing methods, and shows potential for improvement given more training data.

### D.2. Parameter Study: $\theta$

We present a parameter study on the parameter  $\theta$ , the improvement threshold on the mutual information criterion in TU. In our previous experiments, we found the default  $\theta = 0$  to work well, and did not specifically tune  $\theta$ . However, tuning for a larger  $\theta$  could lead to better trade-offs, since small improvements in the quality of the hash mapping may not justify the cost of a full hash table update.

For this study, we vary parameter  $\theta$  from  $-\infty$  to  $\infty$  for all methods (with 32-bit hash codes).  $\theta = -\infty$  reduces to the baseline. On the other hand,  $\theta = \infty$  prevents any updates to the initial hash mapping and hash table, and results in only one hash table update (for the initial mapping) and typically low performance. The performance metric we focus on in this study is the cumulative metric, AUC, since it better summarizes the entire online learning process than the final performance alone.

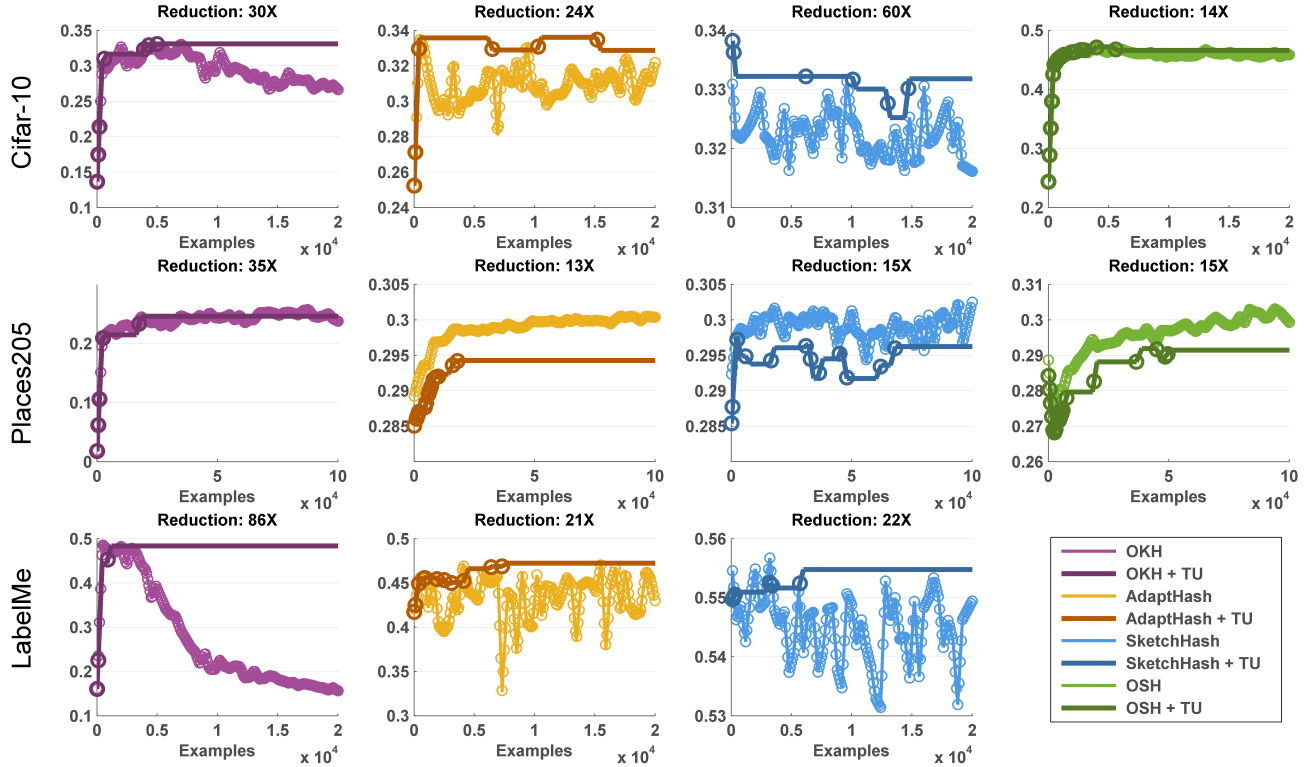


Figure 7: 64-bit experiments: Retrieval mAP vs. number of training examples for four existing online hashing methods on the three datasets, with and without Trigger Update (TU). We use default threshold  $\theta = 0$  for TU. Circles indicate hash table updates, and the ratio of reduction in the number of updates is marked for each graph. TU substantially reduces the number of updates while having a stabilizing effect on the retrieval performance. Note: since the OSH method assumes supervision in terms of class labels, it is not applicable to the unsupervised LabelMe dataset.

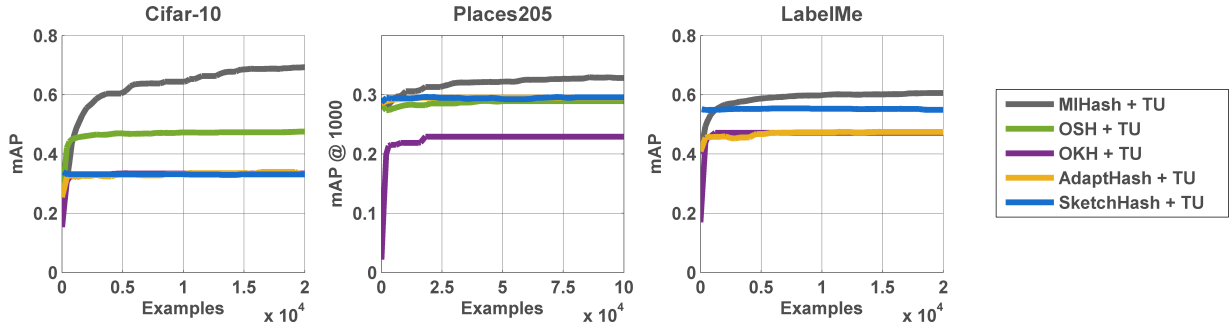


Figure 8: 64-bit experiments: Online hashing performance (mAP) comparison on three datasets, where all methods use the Trigger Update module (TU) with  $\theta = 0$ . Using the mutual information objective, MIHash clearly outperforms other methods. OKH, AdaptHash, and SketchHash perform very similarly on Cifar-10. OSH, AdaptHash, and SketchHash perform very similarly on Places205. Again, the OSH method is not applicable to the unsupervised LabelMe dataset.

We use a custom update schedule for SketchHash: we enforce hash table updates in the early iterations regardless of other criteria, until the number of observed examples reaches the specified size of the “data sketch”, which SketchHash uses to perform a batch hashing algorithm. This was observed to be critical for the performance of SketchHash. Therefore, the number of hash table updates for SketchHash can be greater than 1 even for  $\theta = \infty$ .

We present full results in Tables 4, 5, 6. In all cases, we observe a substantial decrease in the number of hash table updates as  $\theta$  increases. With reasonable  $\theta$  values (typically around 0), the number of hash table updates can be reduced by over an order of magnitude with no loss in AUC. Note that the computation-performance trade-off achieved by the default  $\theta = 0$  is always among the best, thereby in practice it can be used without tuning.

### D.3. Parameter Study: $U$

We simulate a data-agnostic baseline that updates hash tables at a constant rate, using the update interval parameter  $U$ . In Sec. 4,  $U$  is set such that the baseline updates a total of 201 times for all datasets. This ensures that the baseline is never too outdated (compared to 50 checkpoints at which performance is evaluated), but is still fairly infrequent: the smallest  $U$  in this case is 100, which means the baselines process at least 100 training examples before recomputing the hash table. For completeness, here we present results using different values of  $U$ , where all methods again use 32-bit hash codes and the default  $\theta = 0$ .

We used a simple rule that avoids unnecessary hash table updates if the hash mapping itself does not change. Specifically, we do not update if  $\|\Phi_t - \Phi^s\| < 10^{-6}$ , where  $\Phi^s$  is the current snapshot and  $\Phi_t$  is the new candidate. Some baseline entries have fewer updates because of this rule (*e.g.* AdaptHash on Places205). And as explained before, due to the custom update schedule, SketchHash may have more hash table updates than what is suggested by  $U$ .

Please see Tables 7, 8, 9 for the full results. In all experiments, we run three random trials and average the results as mentioned before, and the standard deviation of mAP and AUC scores are less than 0.01. Generally, using smaller  $U$  leads to more updates by both the baselines and methods with TU; recall that  $U$  is also a parameter of TU which specifies the frequency of checking the update criterion. However, methods with the TU module appear to be quite insensitive to the choice of  $U$ , *e.g.* the number of updates for SketchHash with TU on CIFAR-10 only increases by 2x while  $U$  is reduced by 20x, from 1000 to 50. We attribute this to the ability of TU to filter out unnecessary updates. Across different values of  $U$ , TU consistently brings computational savings while preserving/improving online hashing performance, as indicated by final mAP and AUC.

CIFAR-10, 32 bits			
OKH	HT Updates	AUC	$\Delta$ AUC
$\leq -0.1$	201	0.259	–
$-0.01$	190 (5.8x)	0.260	+0.4%
$-10^{-4}$	8.0 (25.1x)	0.287	+10.8%
0	8.0 (25.1x)	0.287	+10.8%
$10^{-4}$	7.7 (26.1x)	0.287	+10.8%
0.01	3.3 (91.2x)	0.280	+8.1%
$\geq 0.2$	1.0 (201x)	0.134	–48.3%
OSH	HT Updates	AUC	$\Delta$ AUC
$\leq -0.01$	201	0.463	–
$-10^{-4}$	39.0 (5.2x)	0.466	+0.6%
0	36.7 (5.5x)	0.466	+0.6%
$10^{-4}$	35.7 (5.6x)	0.466	+0.6%
0.01	6.7 (30x)	0.453	–2.1%
0.1	2.0 (100x)	0.386	–16%
$\geq 0.3$	1.0 (201x)	0.207	–55%
AdaptHash	HT Updates	AUC	$\Delta$ AUC
$\leq -0.1$	201	0.218	–
$-0.01$	68.3 (2.9x)	0.238	+9.2%
$-10^{-4}$	10.3 (19.5x)	0.250	+14.7%
0	10.0 (20.1x)	0.250	+14.7%
$10^{-4}$	10.0 (20.1x)	0.250	+14.7%
0.01	3.3 (60.9x)	0.244	+11.9%
$\geq 0.1$	1.0 (201x)	0.211	–3.3%
SketchHash	HT updates	AUC	$\Delta$ AUC
$\leq -0.01$	201	0.304	–
$-10^{-4}$	9.0 (22.3x)	0.318	+4.6%
$-10^{-6}$	7.3 (27.5x)	0.319	+4.9%
0	7.3 (27.5x)	0.319	+4.9%
$10^{-4}$	7.3 (27.5x)	0.319	+4.9%
0.01	4.3 (46.7x)	0.318	+4.6%
$\geq 0.1$	4.0 (50.3x)	0.314	+3.3%

Table 4: Parameter study on the threshold value  $\theta$  for on-line hashing methods on **CIFAR-10** (32 bits). We report the number of hash table updates, where 100x indicates a 100 times reduction with respect to the baseline. We also report the area under the mAP curve (AUC) and compare to baseline.



Places205, 32 bits			
OKH	HT Updates	AUC	$\Delta$ AUC
$\leq -0.01$	201	0.163	–
$-10^{-4}$	8.3 (24.2x)	0.161	–1.2%
$-10^{-6}$	7.0 (28.7x)	0.161	–1.2%
0	7.0 (28.7x)	0.161	–1.2%
$10^{-6}$	7.0 (28.7x)	0.161	–1.2%
$10^{-4}$	5.7 (35.3x)	0.161	–1.2%
0.01	2.0 (100x)	0.123	–25%
$\geq 0.1$	1.0 (201x)	0.014	–91%
OSH	HT Updates	AUC	$\Delta$ AUC
$\leq -0.001$	201	0.246	–
$-20^{-4}$	101 (2.0x)	0.246	0%
$-10^{-4}$	9.3 (21.6x)	0.236	–4.1%
0	7.0 (28.7x)	0.236	–4.1%
$10^{-4}$	5.7 (35.3x)	0.230	–6.5%
$10^{-3}$	2.7 (74.4x)	0.224	–8.9%
$\geq 0.1$	1.0 (201x)	0.226	–8.1%
AdaptHash	HT Updates	AUC	$\Delta$ AUC
$\leq -0.01$	199.7	0.237	–
$-10^{-4}$	199 (1.0x)	0.237	0%
$-10^{-6}$	9.7 (20.6x)	0.236	–0.4%
0	8.7 (23.0x)	0.236	–0.4%
$10^{-6}$	8.7 (23.0x)	0.235	–0.8%
$10^{-4}$	3.0 (66.6x)	0.235	–0.8%
$\geq 0.01$	1.0 (201x)	0.227	–3.4%
SketchHash	HT Updates	AUC	$\Delta$ AUC
$\leq -0.01$	201	0.237	–
$-10^{-4}$	52.3 (3.8x)	0.238	+0.4%
$-10^{-6}$	15.3 (12.6x)	0.238	+0.4%
0	12.7 (15.8x)	0.236	–0.4%
$10^{-6}$	15.3 (13.1x)	0.238	+0.4%
$10^{-4}$	7.0 (28.7x)	0.239	+0.8%
$\geq 0.01$	2.0 (101x)	0.223	–5.9%

Table 5: Parameter study on the threshold value  $\theta$  for online hashing methods on **Places205** (32 bits). We report the number of hash table updates, where 100x indicates a 100 times reduction with respect to the baseline. We also report the area under the mAP curve (AUC) and compare to baseline.

LabelMe, 32 bits			
OKH	HT Updates	AUC	$\Delta$ AUC
$\leq -0.2$	201	0.198	–
$-0.1$	196 (1.0x)	0.199	+0.5%
$-0.01$	2.7 (74.4x)	0.373	+88%
$-10^{-6}$	2.3 (87.4x)	0.374	+89%
0	2.3 (87.4x)	0.374	+89%
$10^{-6}$	2.3 (87.4x)	0.374	+89%
0.01	2.0 (101x)	0.372	+88%
$\geq 0.6$	1.0 (201x)	0.111	–44%
AdaptHash	HT Updates	AUC	$\Delta$ AUC
$\leq -0.1$	201	0.333	–
$-10^{-6}$	149 (1.3x)	0.330	–0.9%
$-10^{-4}$	9.3 (21.6x)	0.365	+9.6%
$-10^{-2}$	8.7 (23.1x)	0.365	+9.6%
0	5.3 (37.9x)	0.369	+11%
$10^{-6}$	8.7 (23.1x)	0.365	+9.6%
$10^{-4}$	8.3 (24.2x)	0.358	+7.5%
$10^{-2}$	2.7 (74.4x)	0.351	+5.4%
$\geq 0.1$	1 (201x)	0.296	–11%
SketchHash	HT Updates	AUC	$\Delta$ AUC
$\leq -0.1$	201	0.446	–
$-10^{-2}$	195 (1.0x)	0.446	0%
$-10^{-4}$	9.3 (21.6x)	0.460	+3.1%
0	8.7 (23.1x)	0.460	+3.1%
$10^{-4}$	10 (20.1x)	0.459	+2.9%
$10^{-2}$	4.7 (42.8x)	0.446	0%
$\geq 0.1$	4.0 (50.3x)	0.439	–1.6%

Table 6: Parameter study on the threshold value  $\theta$  for online hashing methods on **LabelMe** (32 bits). We report the number of hash table updates, where 100x indicates a 100 times reduction with respect to the baseline. We also report the area under the mAP curve (AUC) and compare to baseline. Note: OSH is not applicable to this unlabeled dataset since it needs supervision in terms of class labels.

CIFAR-10, 32 bits				
Method	TU	HT Updates	Final mAP	AUC (mAP)
OKH, $U = 10$	×	1870	0.238	0.259
	✓	15.6 (119.3x)	0.297	0.293 (+13%)
OKH, $U = 100$	×	201	0.238	0.259
	✓	8 (25.1x)	0.291	0.287 (+10.8%)
OKH, $U = 1000$	×	21	0.238	0.255
	✓	2.6 (8x)	0.282	0.273 (+7%)
OSH, $U = 10$	×	2001	0.480	0.463
	✓	110.7 (18x)	0.483	0.466 (+0.6%)
OSH, $U = 100$	×	201	0.480	0.463
	✓	36.7 (5.4x)	0.483	0.466 (+0.6%)
OSH, $U = 1000$	×	21	0.480	0.454
	✓	11.3 (1.9x)	0.479	0.454
AdaptHash, $U = 10$	×	2001	0.244	0.224
	✓	19.6 (101.7x)	0.267	0.261 (+16%)
AdaptHash, $U = 100$	×	201	0.244	0.224
	✓	10.0 (10.1x)	0.255	0.250 (+11.6%)
AdaptHash, $U = 1000$	×	21	0.244	0.222
	✓	5 (4.2x)	0.252	0.234 (+5%)
SketchHash, $U = 50$	×	400	0.306	0.303
	✓	9 (44.4x)	0.318	0.318 (+5%)
SketchHash, $U = 100$	×	202	0.306	0.304
	✓	7.3 (27.5x)	0.320	0.319 (+4.9%)
SketchHash, $U = 1000$	×	24	0.306	0.305
	✓	4.6 (5.2x)	0.317	0.314 (+2.9%)

Table 7: Online hashing results (32 bits) with different update interval parameters ( $U$ ) on the **CIFAR-10** dataset. All results are averaged from 3 random trials. For the number of hash table updates, we report the reduction ratio (*e.g.* 8x) for TU. For AUC, we report the relative change compared to baseline. Note: SketchHash uses a batch size of 50, therefore the smallest  $U$  is set to 50.

LabelMe, 32 bits				
Method	TU	HT Updates	Final mAP	AUC (mAP)
OKH, $U = 10$	×	2001	0.119	0.200
	✓	8 (250x)	0.382	0.377 (+88.5%)
OKH, $U = 100$	×	201	0.119	0.200
	✓	2.3 (86.2x)	0.380	0.374 (+87%)
OKH, $U = 1000$	×	21	0.119	0.193
	✓	2 (10.5x)	0.373	0.357 (+85%)
AdaptHash, $U = 10$	×	2001	0.318	0.319
	✓	12.6 (157.9x)	0.380	0.371 (+16.3%)
AdaptHash, $U = 100$	×	201	0.318	0.318
	✓	8.6 (23.1x)	0.379	0.365 (+14.7%)
AdaptHash, $U = 1000$	×	21	0.318	0.317
	✓	5 (4.2x)	0.343	0.337 (+6.3%)
SketchHash, $U = 50$	×	400	0.445	0.447
	✓	9.6 (41.6x)	0.461	0.460 (+2%)
SketchHash, $U = 100$	×	202	0.445	0.446
	✓	8.67 (23.2x)	0.462	0.460 (+3.1%)
SketchHash, $U = 1000$	×	24	0.445	0.445
	✓	8.3 (2.8x)	0.456	0.455 (+2%)

Table 8: Online hashing results (32 bits) with different update interval parameters ( $U$ ) on the **LabelMe** dataset. All results are averaged from 3 random trials. For the number of hash table updates, we report the reduction ratio (*e.g.* 8x) for TU. For AUC, we report the relative change compared to baseline. Note: since LabelMe is an unsupervised dataset, the OSH method is not applicable since it requires supervision in the form of class labels.

Places205, 32 bits				
Method	TU	HT Updates	Final mAP	AUC (mAP)
OKH, $U = 50$	×	2001	0.182	0.163
	✓	8 (250.1x)	0.173	0.169 (+3.7%)
OKH, $U = 500$	×	201	0.182	0.163
	✓	7 (28.7x)	0.165	0.161 (-1.2%)
OKH, $U = 5000$	×	21	0.182	0.156
	✓	2 (10.5x)	0.157	0.148 (-5.1%)
OSH, $U = 50$	×	2001	0.248	0.246
	✓	25 (80x)	0.239	0.238 (-3%)
OSH, $U = 500$	×	201	0.248	0.246
	✓	7 (28.7x)	0.236	0.236 (-4.0%)
OSH, $U = 5000$	×	21	0.248	0.245
	✓	2 (10.5x)	0.234	0.233 (-4%)
AdaptHash, $U = 50$	×	823.7	0.238	0.237
	✓	26.6 (30.8x)	0.236	0.236 (-0.4%)
AdaptHash, $U = 500$	×	200	0.238	0.237
	✓	8.6 (23.0x)	0.236	0.236 (-0.4%)
AdaptHash, $U = 5000$	×	21	0.238	0.237
	✓	3 (7x)	0.236	0.236 (-0.4%)
SketchHash, $U = 50$	×	2000	0.238	0.235
	✓	19.3 (103.4x)	0.236	0.235 (0%)
SketchHash, $U = 500$	×	202	0.237	0.235
	✓	15.3 (13.1x)	0.240	0.238 (+1.2%)
SketchHash, $U = 5000$	×	22	0.235	0.235
	✓	6.6 (3.2x)	0.239	0.238 (+1.2%)

Table 9: Online hashing results (32 bits) with different update interval parameters ( $U$ ) on the **Places205** dataset. All results are averaged from 3 random trials. For the number of hash table updates, we report the reduction ratio (e.g. 8x) for TU. For and AUC, we report the relative change compared to baseline.